

# Highly efficient optical coupling and transport phenomena in chains of dielectric microspheres

Zhigang Chen and Allen Taflove

*Department of Electrical and Computer Engineering, Northwestern University, Evanston, Illinois 60208*

Vadim Backman

*Department of Biomedical Engineering, Northwestern University, Evanston, Illinois 60208*

Received September 6, 2005; revised October 9, 2005; accepted October 11, 2005

Using the generalized multiparticle Mie theory, we investigate optical coupling and transport through chains of dielectric microspheres. We identify two distinct coupling mechanisms of optical transport in terms of the coupling efficiency between neighboring microspheres, namely, evanescent coupling and nanojet coupling. We demonstrate that perfect whispering gallery mode propagation through a chain of evanescently coupled microspheres can be achieved. However, optical coupling and transport through a chain of nanojet-inducing microspheres is less efficient due to the radiative nature of photonic nanojets. Understanding these two optical coupling mechanisms is critical for selecting appropriate microspheres to build coupled resonator optical waveguides and other photon-manipulation devices for effective and low-loss guiding of photons.

© 2006 Optical Society of America

OCIS codes: 230.7370, 230.5750, 230.3990, 290.4020, 290.4210.

During the past two decades there has been considerable interest in the optical properties of dielectric microcylinders and microspheres.<sup>1–5</sup> Because they exhibit whispering gallery mode (WGM) resonances with high quality factors, they are the most natural choice for the unit to be employed in tight-binding photonic devices such as coupled resonator optical waveguides.<sup>6–8</sup> Successful light propagation by WGMs through a chain of coupled cylinder resonators has been studied.<sup>4</sup> In the case of sphere resonators, a regime of strong coupling between two microspheres with marked normal mode splitting has been observed.<sup>9</sup> This ensures the feasibility of tight-binding manipulation of light waves in a microstructure composed of touching spheres. In addition, long-range propagation effects were observed in slightly disordered chains of polystyrene microspheres, and the corresponding optical transport properties were interpreted in terms of coupling between WGM resonances with random detuning.<sup>10</sup> However, the achieved coupling efficiency has been low for chains of polystyrene microspheres that have a refractive index of  $\sim 1.59$ . Recent discussions on the phenomenology of photonic nanojets<sup>3</sup> emerging from the shadow-side surface of a dielectric microcylinder or a microsphere may help shed some light on the coupling efficiency between neighboring microspheres. It is critical to note that photonic nanojets contain not only evanescent fields but also strong radiative-mode components. As a result, optical coupling and transport through a chain of nanojet-inducing microspheres should be different from that through a chain of evanescent-field-inducing microspheres.

In this Letter, using the generalized multiparticle Mie (GMM) theory,<sup>11</sup> we investigate optical transport through chains of dielectric microspheres. We identify two distinct coupling mechanisms of optical transport between the chain spheres, namely, evanescent and nanojet coupling. In the case of evanes-

cent coupling, a chain consists of evanescent-field-inducing microspheres that operate as a series of evanescently coupled microlenses. Optical transport is achieved through evanescent-wave coupling between neighboring spheres. In a chain of nanojet-inducing microspheres, the constituent spheres are nonevanescently coupled due to the radiative nature of photonic nanojets. We demonstrate that perfect WGM propagation through a chain of evanescently coupled microspheres can be achieved. However, for a chain of nanojet-inducing microspheres, perfect optical coupling and transport is not possible due to the radiative nature of photonic nanojets.

It is clear that for visible light a microsphere can be used to focus an incident plane wave. Depending on its refractive index, the focus point can be inside or outside the sphere. However, when the focus point is just at the surface of the sphere, the full width at half-maximum of the focus point becomes smaller than the wavelength over a distance of a few wavelengths.<sup>3</sup> This unique focus point has been termed a photonic nanojet<sup>3</sup> based on its appearance. A typical nanojet is shown in Fig. 1(a), which shows the electric field intensity distribution of a plane-wave-illuminated ( $\lambda=400$  nm) sphere of diameter  $d=3$   $\mu\text{m}$  and refractive index  $m=1.59$  in free space. Here, the calculation of the nanojet is conducted using the Lorentz–Mie theory. This nanojet is distinguished from the well-known evanescent field appearing at the surface of a sphere with a relatively high refractive index. For comparison, an example of the evanescent field generated at the surface of a microsphere that has a refractive index of 1.8 is shown in Fig. 1(b). The optical power within such a microsphere is totally internally reflected and can be tunneled out of it through evanescent coupling. Comparing Fig. 1(a) with Fig. 1(b), it is evident that the photonic nanojet in Fig. 1(a) possesses not only evanescent fields but also radiative-mode components. It

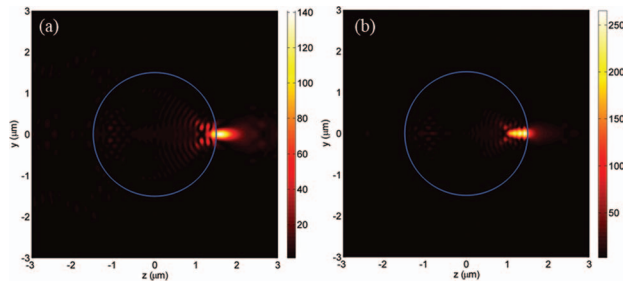


Fig. 1. (a) Visualization of a photonic nanojet emerging at the shadow-side surface (blue circle) of a dielectric microsphere of diameter  $d=3 \mu\text{m}$  that has a refractive index of 1.59 and is illuminated by a plane wave ( $\lambda=400 \text{ nm}$ ). The electric field intensity (normalized to the incident intensity) is visualized on the meridian plane. (b) Visualization of an evanescent wave emerging at the shadow-side surface (blue circle) of a dielectric microsphere of diameter  $d=3 \mu\text{m}$  that has a refractive index of 1.8 and is illuminated by a plane wave ( $\lambda=400 \text{ nm}$ ).

is the radiative nature of the nanojet that renders the optical coupling between nanojet-coupled microspheres less efficient.

We now provide quantitative studies to demonstrate two distinct optical coupling mechanisms for chains of dielectric microspheres, namely, one of radiative nature and one of interacting WGMs. To obtain quantitative data, we apply the GMM theory.<sup>11</sup> We assume that an incident plane wave of unity amplitude is linearly polarized along the  $x$  axis and propagates along the  $z$  axis. The origin of the primary coordinate system is taken at the center of the  $j_0$ th sphere. In the GMM theory, the internal electric fields of each sphere in the primary coordinate system are given by  $\mathbf{E}_{\text{int}}(j, j_0) = -\sum_{n=1}^{\infty} \sum_{m=-n}^n i E_{mn} [d_{mn}^{j, j_0} \mathbf{N}_{mn}^{(1)} + c_{mn}^{j, j_0} \mathbf{M}_{mn}^{(1)}]$ ,<sup>11</sup> where  $\mathbf{M}_{mn}^{(1)}$  and  $\mathbf{N}_{mn}^{(1)}$  are the vector spherical wave functions (the superscripts denote the kind of spherical Bessel function),  $E_{mn} = i^n (2n+1)(n-m)!/(n+m)!$ ,  $c_{mn}^{j, j_0}$  and  $d_{mn}^{j, j_0}$  are the internal coefficients, and  $(j, j_0)$  represents the internal field of the  $j$ th sphere expanded in the primary  $j_0$ th coordinate system. The internal intensity of each sphere is defined by  $I(j, j_0) = |\mathbf{E}_{\text{int}}(j, j_0)|^2$ . For simplicity and without losing the generality of the problem, we study two chains of five touching spheres. The first chain consists of nanojet-inducing dielectric microspheres, as shown in Fig. 1(a), and the second chain consists of evanescent-field-inducing dielectric microspheres that have a higher refractive index, as shown in Fig. 1(b). These two sphere chains are different in terms of only the refractive index.

Figure 2(a) shows the intensity distribution of each constituent sphere of the first chain consisting of microspheres that have a refractive index of 1.59 and induce photonic nanojets as shown in Fig. 1(a). From Fig. 2(a), we see that a WGM resonance ( $\lambda=429.069 \text{ nm}$ ) is weakly excited within each sphere by the evanescent-field component of the nanojet, and its propagation through the sphere chain is achieved via evanescent coupling. However, due to the radiative nature of the nanojet, optical coupling between neighboring spheres is not efficient. The radiative-mode component of the nanojet of each

sphere is not well coupled to its next neighbor. A major part of this component is scattered by the next nearest sphere and lost to the surrounding medium. To better show the coupling efficiency between neighboring spheres, we calculate the peak intensity of each sphere along the chain and plot it as a function of the distance between centers of the constituent spheres. This calculation is visualized in Fig. 2(b). We see that the incident light can propagate efficiently only as far as the third sphere. The intensities within the fourth and fifth spheres go down dramatically.

To achieve better optical transport, we can use a chain of evanescently coupled microspheres. Such a

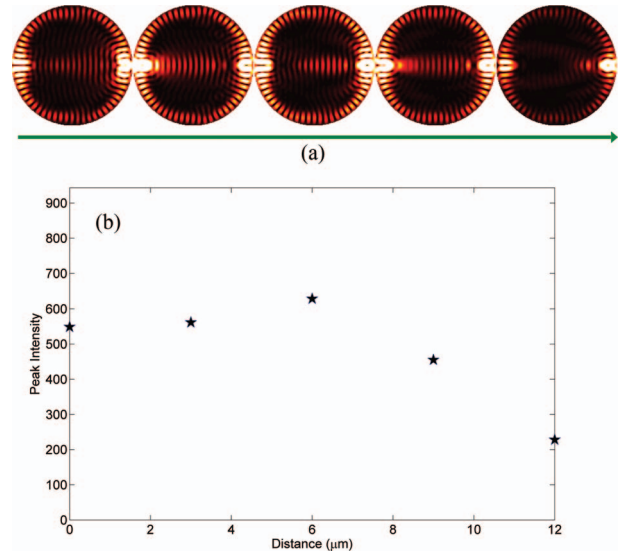


Fig. 2. (a) Electric field intensity distribution of a chain of five touching microspheres that have a refractive index of 1.59 and a diameter of  $3 \mu\text{m}$ . Light of wavelength  $\lambda = 429.069 \text{ nm}$  propagates from left to right. (b) Peak intensity of each constituent sphere as a function of the distance between their centers.

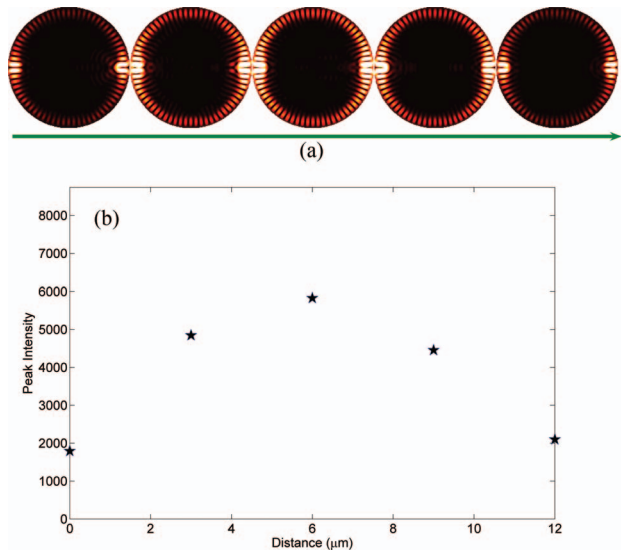


Fig. 3. (a) Electric field intensity distribution of a chain of five touching microspheres that have a refractive index of 1.8 and a diameter of  $3 \mu\text{m}$ . Light of wavelength  $\lambda = 430.889 \text{ nm}$  propagates from left to right. (b) Peak intensity of each constituent sphere as a function of the distance between their centers.

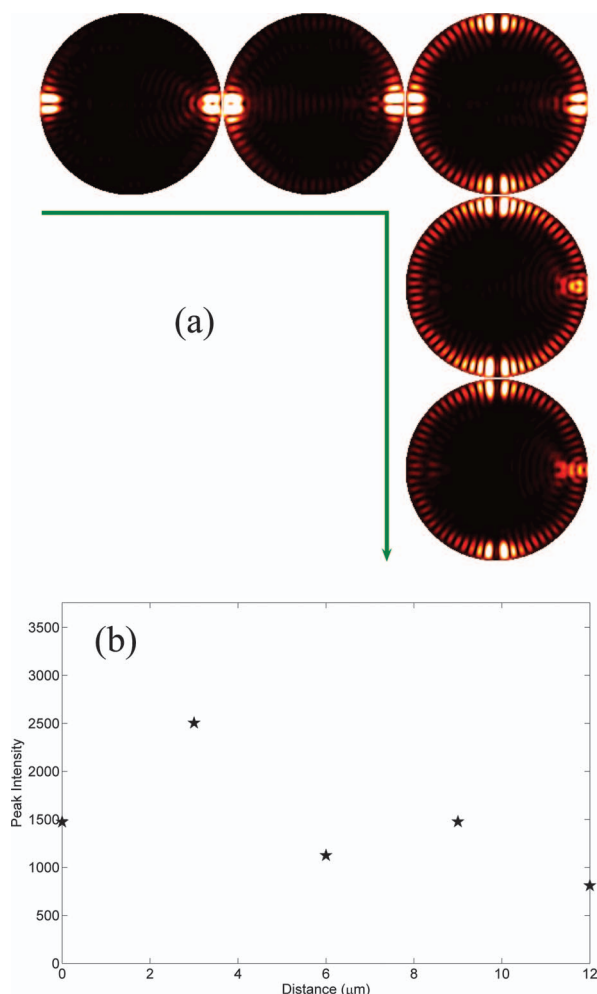


Fig. 4. (a) Electric field intensity distribution of a bent chain of five touching microspheres with a rake of  $90^\circ$  that have a refractive index of 1.8 and a diameter of  $3 \mu\text{m}$ . Light of wavelength  $\lambda = 431 \text{ nm}$  propagates from left to right. (b) Peak intensity of each constituent sphere as a function of the distance between their centers.

chain can be built using the microsphere shown in Fig. 1(b), which has a refractive index of 1.8. Figure 3(a) shows the intensity distribution of such a sphere chain. We see that a pure WGM resonance ( $\lambda = 430.889 \text{ nm}$ ) is excited within each sphere of the chain. The optical fields within each sphere are predominantly WGM resonances, and these pure WGM resonances are perfectly coupled between neighboring spheres via evanescent coupling. Figure 3(b) shows the peak intensity within each sphere along the chain. We see that the incident light can propagate efficiently as far as the end sphere. The incident light is transported perfectly from the first sphere to the last sphere, and the intensity distribution of the last sphere is nearly identical to that of the first sphere. Therefore, highly efficient optical transport is achieved in such a sphere chain.

We have further investigated optical transport through a bent chain of microspheres with a rake of  $90^\circ$ , as shown in Fig. 4(a). This bent chain consists of

five touching microspheres shown in Fig. 1(b). Figure 4(a) shows the intensity distribution of such a chain illuminated by a plane wave ( $\lambda = 431 \text{ nm}$ ). Figure 4(a) reveals that efficient WGM coupling can take place even across the abrupt direction change of  $90^\circ$ . Therefore, the incident light can be efficiently transported over a rake to the end sphere via evanescent coupling. Figure 4(b) shows the peak intensity of each sphere along the chain. We see that the peak intensity of the end sphere in Fig. 4 retains a reasonably high level comparable to that of the first sphere. We note that these results are consistent with those obtained by Yannopapas *et al.* for a bent waveguide in photonic crystals consisting of nonoverlapping spheres.<sup>12</sup>

In conclusion, we have investigated optical coupling and transport through a chain of touching dielectric microspheres by use of the GMM theory. Two coupling mechanisms are identified for such a sphere chain. The first coupling mechanism, nanojet coupling, is by no means efficient because of the radiative nature of nanojets emerging at the shadow-side surface of a microsphere. However, highly efficient optical coupling can be achieved by using a chain of evanescently coupled microspheres that have a relatively high refractive index and induce evanescent fields at their shadow-side surfaces. Understanding these two coupling mechanisms is critical for selecting the underlying microspheres from which to build coupled resonator optical waveguides and other photon-manipulation devices for highly efficient guided light-wave propagation over a long distance.

This work was supported in part by NSF grant BES-0522639. We thank Y.-L. Xu for making his FORTRAN codes available to the public. Z. Chen's e-mail address is zhigang@iastate.edu.

## References

1. J. F. Owen, R. K. Chang, and P. W. Barber, *Opt. Lett.* **6**, 540 (1981).
2. D. S. Benincasa, P. W. Barber, J.-Z. Zhang, W.-F. Hsieh, and R. K. Chang, *Appl. Opt.* **26**, 1348 (1987).
3. Z. Chen, A. Taflove, and V. Backman, *Opt. Express* **12**, 1214 (2004).
4. S. Deng, W. Cai, and V. N. Astratov, *Opt. Express* **12**, 6468 (2004).
5. R. K. Chang and A. J. Campillo, *Optical Processes in Microcavities* (World Scientific, 1996).
6. N. Stefanou and A. Modinos, *Phys. Rev. B* **57**, 12 127 (1998).
7. E. Lidorikis, M. M. Sigalas, E. N. Economou, and C. M. Soukoulis, *Phys. Rev. Lett.* **81**, 1405 (1998).
8. A. Yariv, Y. Xu, R. K. Lee, and A. Scherer, *Opt. Lett.* **24**, 711 (1999).
9. T. Mukaiyama, K. Takeda, H. Miyazaki, Y. Jimba, and M. Kuwata-Gonokami, *Phys. Rev. Lett.* **82**, 4623 (1999).
10. V. N. Astratov, J. P. Franchak, and S. P. Ashili, *Appl. Phys. Lett.* **85**, 5508 (2004).
11. Y.-L. Xu, *Appl. Opt.* **34**, 4573 (1995).
12. V. Yannopapas, A. Modinos, and N. Stefanou, *Phys. Rev. B* **65**, 235201 (2002).